



Scholars Research Library

Der Pharmacia Lettre, 2015, 7 (6):125-140
(<http://scholarsresearchlibrary.com/archive.html>)



Chemical composition, adsorption proprieties and corrosion inhibition on mild steel of *Mentha rotundifolia* L. essential oil from Morocco

A. Ansari¹, M. Znini¹, A. Laghchimi¹, J. Costa², P. Ponthiaux³ and L. Majidi^{1*}

¹Université My Ismail, Laboratoire des Substances Naturelles & Synthèse et Dynamique Moléculaire, Faculté des Sciences et Techniques, Errachidia, Morocco

²Université de Corse, CNRS-UMR 6134, Laboratoire de Chimie des Produits Naturels, Corti, France

³Centrale-Supélec, Grande Voie des Vignes, Châtenay-Malabry, France

ABSTRACT

The analysis of *Mentha rotundifolia* L. essential oil by Gas Chromatography (GC) and Gas Chromatography-Mass Spectrometry (GC/MS) allowed the identification of 25 components, which accounted for 94.3% of the total oil. Pulegone (69.1%) and menthone (18.5%) were identified as main compounds. The inhibitive effect of this essential oil on the corrosion of mild steel in 1M HCl solution has been investigated by weight loss measurement as well as potentiodynamic polarization and electrochemical impedance spectroscopy (EIS) techniques. The gravimetric results indicate that MR oil exhibits good inhibition efficiency in 1M HCl solution. The effect of temperature on the corrosion behavior of mild steel was studied in the range of 303–333K. Polarization measurements showed that the studied inhibitor is mixed type with significant reduction of cathodic and anodic current densities. Electrochemical impedance spectroscopy measurements revealed that the charge transfer resistance increases with increase in the concentration of essential oil. Various activation parameters such as activation energy, activation enthalpy and activation entropy are evaluated and discussed. Adsorption thermodynamic parameters are also computed. Linearity of Langmuir isotherm adsorptions indicated the monolayer formation of inhibitor on mild steel surface.

Keywords *Mentha rotundifolia*, Essential oil, Mild steel, Corrosion inhibition,

INTRODUCTION

Corrosion is a major destructive process affecting the performance of metallic materials in applications in many industrial sectors. It is a naturally occurring phenomenon commonly defined as deterioration of metal surfaces caused by the reaction with the surrounding environmental conditions [1]. To prevent or minimize internal corrosion in these systems, the use of inhibitors is one of the best methods of protecting metals against corrosion, especially in acid descaling bathes [2].

In recent years, Natural compounds extracted from plant, such as essential oils, have been explored as corrosion inhibitors because to their bio-degradability, eco-friendliness, low cost and easy availability [3]. The inhibition performance of essential oils is normally ascribed to the presence in their composition of complex organic species including oxygenated monoterpenes and sesquiterpenes as major constituents. These organic compounds usually contain polar functions with oxygen atoms as well as those with conjugated double bonds or aromatic rings in their molecular structures, which may act as green corrosion inhibitors for mild steel dissolution due to the chelating action and the formation of a physical blocking barrier on the metal surface [4].

Much work has been conducted to study the inhibition by essential oils on the corrosion of steel in acidic media and have been found to be very efficient corrosion inhibitors for mild steel in these acid media [4-11].

Mentha rotundifolia, commonly known as “pineapple mint”, is an herbaceous and aromatic plant species belongs to the family *Lamiaceae*. It is considered to be a hybrid derived from a cross between *Mentha longifolia* and *Mentha suaveolens* [12], whereas, some authors have considered *M. rotundifolia* as a synonym of *M. suaveolens* [13]. It is very widely distributed around the Mediterranean basin, in America, in occidental, in Asia and in northern Africa. In Morocco, this plant, which locally known such as "Timarssad, grows wildly in humid region both in the plains than in the mountains. It was used for their flavours in cooking and in folk medicine for a wide range of actions: tonic, stimulative, stomachic, carminative, analgesic, holeritic, antispasmodic, anti-inflammatory, sedative, hypotensive, antibacterial and insecticidal [14,15].

In the present study, the inhibitive effects of components from *Mentha rotundifolia* essential oil on corrosion of mild steels in hydrochloric acid solution were investigated for the first time. For this purpose, the oil chemical composition has been studied using GC (Gas Chromatography) and GC-MS (Gas Chromatography-Mass Spectrometry). The investigation of corrosion parameters was performed by weight loss, electrochemical polarization measurements and electrochemical impedance spectroscopy. The effect of temperature was also studied and discussed.

MATERIALS AND METHODS

Plant material

The aerial parts of *Mentha rotundifolia* were harvested in April 2011 (full bloom) in Errachidia located at the south-east of Morocco. Voucher specimen was deposited in the herbarium of Faculty of Sciences and Technology of Errachidia (Morocco).

Essential oil isolation

The dried vegetal material (100 g) were water-distilled (3h) using a Clevenger-type apparatus according to the method recommended in the European Pharmacopoeia [16]. The yield of essential oil was 0.6%.

GC analysis

GC analysis were carried out using a Perkin-Elmer Autosystem XL GC apparatus equipped with dual flame ionization detection (FID) system and fused-silica capillary columns (60 m×0.22 mm I.D., film thickness 0.25 µm), Rtx-1 (polydimethylsiloxane) and Rtx-wax (polyethyleneglycol). The oven temperature was programmed from 60°C to 230°C at 2°C/min and then held isothermally at 230°C for 35 min. Injector and detector temperature was maintained at 280°C. Samples were injected in the split mode (1/50), using helium as carrier gas (1 ml/min); the injection volume was 0.2 µL of pure oil. Retention indices (RI) of compounds were determined relative to the retention times of series of n-alkanes (C₅-C₃₀) with linear interpolation, using the Van den Dool and Kratz equation [17] and software from Perkin-Elmer. Component relative concentrations were calculated based on GC peak areas without using correction factors.

GC-MS analysis

Samples were also analysed using a Perkin-Elmer Turbo mass detector (quadrupole), coupled to a Perkin-Elmer Autosystem XL, equipped with fused-silica capillary columns Rtx-1 and Rtx-Wax. Carrier gas: helium (1 mL/min), ion source temperature: 150°C, oven temperature programmed from 60°C to 230°C at 2°C/min and then held isothermally at 230°C (35 min), injector temperature: 280°C, energy ionization: 70 eV, electron ionization mass spectra were acquired over the mass range 35-350 Da, split: 1/80, injection volume: 0.2 µL of pure oil.

Identification of components

The methodology carried out for identification of individual components was based on: i) comparison of calculated retention indices (RI), on polar and apolar columns, with those of authentic compounds or literature data [18]; ii) computer matching with commercial mass spectral libraries [19] and comparison of mass spectra with those of our own library of authentic compounds or literature data [18,20].

Preparation of materials

Mild steel coupons containing 0.09 wt.% (P), 0.38 wt.% (Si), 0.01 wt.% (Al), 0.05 wt.% (Mn), 0.21 wt.% (C), 0.05 wt.% (S) and the remainder iron (Fe) used for weight loss measurements. The surface preparation of the mild steel coupons (2 cm x 2 cm) was carried out with emery papers by increasing grades (400, 600 and 1200 grit size), then degreased with AR grade ethanol and dried at room temperature before use. The aggressive solutions of 1 M HCl was prepared by dilution of analytical grade 37% HCl with double distilled water. The concentration range of the MR oil was 0.25-2 g/L. This concentration range was chosen upon the maximum solubility of MR oil. All reagents used for the study were of analytical grade.

Electrochemical studies

Electrochemical measurements were carried out in a conventional three-electrode electrolysis cylindrical Pyrex glass cell. The working electrode (WE) in the form of disc cut from steel has a geometric area of 1 cm^2 and is embedded in polytetrafluoroethylene (PTFE). A saturated calomel electrode (SCE) and a disc platinum electrode were used respectively as reference and auxiliary electrodes, respectively. The temperature was thermostatically controlled at 303 K. The WE was abraded with silicon carbide paper (grade P1200), degreased with AR grade ethanol and acetone, and rinsed with double-distilled water before use.

Potentiodynamic polarization curves

Polarization curves studies were carried out using EG&G Instruments potentiostat-galvanosta (Model 263A) at 303 K without and with addition of various concentrations of MR oil (0.25-2 g/L) in 1 M HCl solution at a scan rate of 0.5 mV/sec. Before recording the cathodic polarisation curves, the mild steel electrode is polarised at -800 mV for 10 min. For anodic curves, the potential of the electrode is swept from its corrosion potential after 30 min at free corrosion potential, to more positive values. The test solution is deaerated with pure nitrogen. Gas bubbling is maintained through the experiments.

In the case of polarization method the relation determines the inhibition efficiency (E_i %):

$$E_i \% = \frac{I_{\text{corr}} - I_{\text{corr(inh)}}}{I_{\text{corr}}} \times 100 \quad (1)$$

where I_{corr} and $I_{\text{corr(inh)}}$ are the corrosion current density values without and with the inhibitor, respectively, obtained by extrapolation of cathodic and anodic Tafel lines to the corrosion potential.

Electrochemical impedance spectroscopy (EIS)

The electrochemical impedance spectroscopy (EIS) measurements were carried out with the electrochemical system which included a digital potentiostat model Volta lab PGZ 100 computer at E_{corr} after immersion in solution without bubbling, the circular surface of mild steel exposing of 1 cm^2 to the solution were used as working electrode. After the determination of steady-state current at a given potential, sine wave voltage (10 mV) peak to peak, at frequencies between 100 kHz and 10 mHz were superimposed on the rest potential. Computer programs automatically controlled the measurements performed at rest potentials after 30 min of exposure.

The impedance diagrams are given in the Nyquist representation. Values of R_t and C_{dl} were obtained from Nyquist plots. The charge-transfer resistance (R_t) values are calculated from the difference in impedance at lower and higher frequencies, as suggested by Tsuru et al. [21]. The inhibition efficiency got from the charge-transfer resistance is calculated by the following relation:

$$E_{R_t} \% = \frac{R'_t - R_t}{R'_t} \times 100 \quad (2)$$

Where R_t and R'_t are the charge-transfer resistance values without and with inhibitor respectively. R_t is the diameter of the loop.

The double layer capacitance (C_{dl}) and the frequency at which the imaginary component of the impedance is maximal ($-Z_{\text{max}}$) are found determined by Eq. (3):

$$C_{dl} = \frac{1}{\omega \cdot R_t} \quad \text{where } \omega = 2 \pi \cdot f_{\text{max}} \quad (3)$$

Impedance diagrams are obtained for frequency range 100 KHz – 10 mHz at the open circuit potential for mild steel in 1 M HCl in the presence and absence of MR oil.

Weight loss measurements

Weight loss tests were carried out in a double walled glass cell equipped with a thermostat-cooling condenser. The solution volume was 100 mL with and without the presence of different concentrations of MR oil ranging from 0.25 to 2 g/L at various temperatures (303-343 K). After 6 h of immersion, the specimens of steel were carefully washed in double-distilled water, dried and then weighed. The rinse removed loose segments of the film of the corroded samples. Triplicate experiments were performed in each case and the mean value of the weight loss is reported using an analytical balance (precision $\pm 0.1 \text{ mg}$). Weight loss allowed us to calculate the mean corrosion rate as expressed in $\text{mg} \cdot \text{cm}^{-2} \cdot \text{h}^{-1}$.

The corrosion rate (W_{corr}) and inhibition efficiency E_w (%) were calculated according to the Eqs. (4) and (5) respectively:

$$W = \frac{\Delta m}{St} \quad (4)$$

$$E_w \% = \frac{W_{\text{corr}} - W_{\text{corr(inh)}}}{W_{\text{corr}}} \times 100 \quad (5)$$

where Δm (mg) is the specimen weight before and after immersion in the tested solution, W_{corr} and $W_{\text{corr(inh)}}$ are the values of corrosion weight losses ($\text{mg}/\text{cm}^2 \cdot \text{h}$) of mild steel in uninhibited and inhibited solutions, respectively, S is the area of the mild steel specimen (cm^2) and t is the exposure time (h).

The degree of surface coverage was calculated using:

$$\theta = \frac{W_{\text{corr}} - W_{\text{corr(inh)}}}{W_{\text{corr}}} \quad (6)$$

where θ is surface coverage; $W_{\text{corr(inh)}}$ is corrosion rate for steel in presence of inhibitor, W_{corr} is corrosion rate for steel in the absence of inhibitor.

RESULTS AND DISCUSSION

Essential oil composition

Analysis of *Mentha rotundifolia* essential oil (MR oil) was carried out by GC and GC-MS using the methodologies described in the section 2. Twenty-four components amounting to 96.6% of the total oil composition were identified by comparison of their electron ionization-mass spectra (EI-MS) and their retention indices (RI) with those of our own authentic compound library (Table 1). These compounds including five monoterpene hydrocarbons (3, 5-7, 9), eight oxygenated monoterpenes (10-17), four sesquiterpene hydrocarbons (18-21), three oxygenated sesquiterpenes (22-24) and four linear non-terpenic compounds (1, 2, 4, 8).

The chemical composition of the MR oil was strongly dominated by oxygenated monoterpenes (92.3% of the total oil) with pulegone **15** (69.1%) and menthone **12** (18.5%) as major components. It should be noted that monoterpene (1.7%) and sesquiterpene hydrocarbons (0.8%) were represented only slightly in this essential oil. Oxygenated sesquiterpenes and other oxygenated aliphatic components amounted to 0.7% and 1.1% of total oil, respectively.

Various chemotypes of *M. rotundifolia* essential oils have been previously reported according to the geographical origins of samples. For instance, chemical compositions from plant material of various countries of the world showed piperitenone oxide [13,22,23], pipéritone oxide [13,24], menthol [15] and piperitol [25] as major components of essential oils. This chemical variability of *M. rotundifolia* may be explained by several factors, such as plant genotype, geographical condition, season and agronomic condition, which act on loci terpene biosynthesis pathways and contribute to the emergence of different chemical profiles [26].

Potentiodynamic polarization curves

Potentiodynamic anodic and cathodic polarization plots for mild steel specimens in 1 M HCl solution in the absence and presence of different concentrations of MR oil at 25°C are shown in Fig. 1. The respective kinetic parameters including corrosion current density (I_{corr}), corrosion potential (E_{corr}), cathodic and anodic Tafel slopes (β_c , β_a) and inhibition efficiency (IE%) are given in Table 2.

Table 1 Chemical composition of *Mentha rotundifolia* essential oil from Morocco

N ^a	Components	RI l ^b	RI a ^c	RI p ^d	% ^e
1	<i>trans</i> -2-Hexenal		824		0.2
2	Isobutyl isobutyrate		900	1087	0.4
3	α -Pinene	936	930	1021	0.4
4	1-Octen-3-ol	962	961	1441	0.4
5	Sabinene	973	964	1118	0.2
6	β -Pinene	978	970	1107	0.4
7	Myrcene	987	981	1154	0.2
8	3-Methylbutyl isobutyrate	994	1001	1172	0.1
9	Limonene	1025	1021	1195	0.5
10	1,8-Cineol	1024	1021	1206	0.2
11	Linalol	1086	1084	1536	0.2
12	Menthone	1136	1137	1455	18.5
13	Isomenthone	1146	1145	1479	0.7
14	<i>cis</i> -Isopulegone	1148	1151	1660	2.3
15	Pulegone	1215	1221	1633	69.1
16	Piperitone	1226	1229	1714	0.3
17	Piperitenone	1318	1310	1894	1.0
18	α -Copaene	1379	1374	1482	0.2
19	(E)- β -Caryophyllene	1421	1415	1584	0.2
20	Germacrene D	1479	1473	1700	0.3
21	δ -Cadinene	1520	1513	1740	0.1
22	Spathulenol	1572	1561	2125	0.3
23	Caryophyllene oxide	1578	1566	1956	0.2
24	τ -Cadinol	1633	1623	2145	0.2
Total identified					96.6
Monoterpene Hydrocarbons					1.7
Oxygenated Monoterpenes					92.3
Sesquiterpene Hydrocarbons					0.8
Oxygenated Sesquiterpenes					0.7
Oxygenated and aliphatic components					1.1

^a Order of elution are given on apolar column (Rtx-1);

^b RI l = retention indices on the apolar column (Rtx-1) in literature;

^c RI a = retention indices on the apolar column (Rtx-1) ;

^d RI p = retention indices on the polar column (Rtx-Wax);

^e Relative percentages of components (%) are calculated on GC peak areas on the apolar column (Rtx-1) except for components with identical RI a (concentration are given on the polar column).

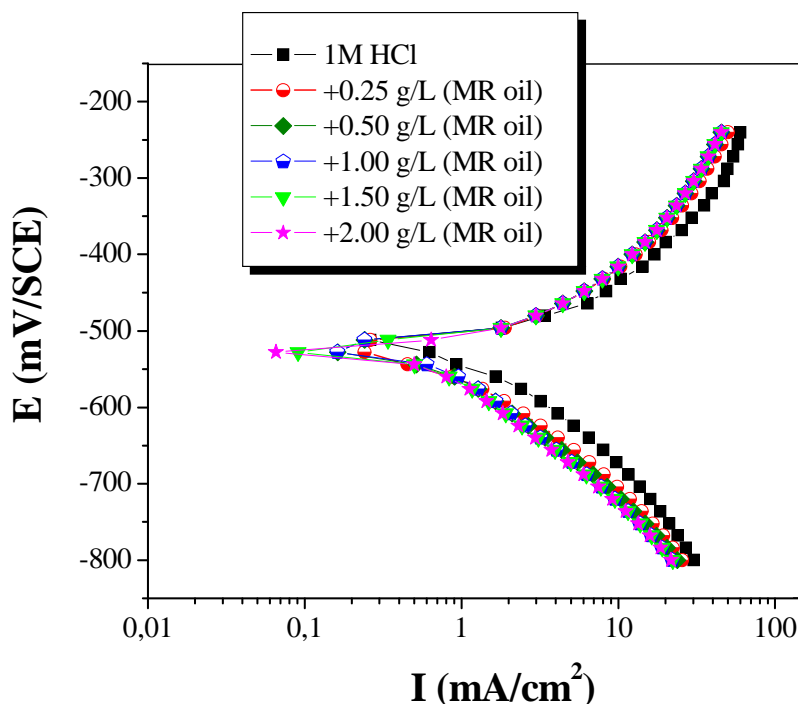


Fig. 1. Anodic and cathodic polarization curves of mild steel in solutions of 1 M HCl in the presence and absence of different concentrations of *Mentha rotundifolia* essential oil.

It is clear from Fig. 1 that the addition of MR oil has an inhibitive effect in the both anodic and cathodic parts of the polarization curves. This indicates a modification of the mechanism of cathodic hydrogen evolution as well as anodic dissolution of steel, which suggest that inhibitor powerfully inhibits the corrosion process of mild steel, and its ability as corrosion inhibitor is enhanced as its concentration is increased. In addition, the parallel cathodic Tafel curves in Fig. 1 show that the hydrogen evolution is activation-controlled and the reduction mechanism is not affected by the presence of this inhibitor.

Table 2 Polarization parameters for the mild steel in 1 M HCl containing different concentrations of *Mentha rotundifolia* essential oil

C (g/L)	E_{corr} (mV/SCE)	I_{corr} (mA/cm ²)	$-\beta_c$ (mV)	β_a (mV)	$E_1\%$
0	-512.12	2.406	226.6	194.1	--
0.25	-527.8	1.456	174.7	146.4	39.49
0.50	-528	1.183	174.3	146.6	50.84
1.00	-526.91	0.743	175.7	142.2	69.14
1.50	-527	0.578	174	142	75.97
2.00	-527.84	0.526	176.1	144.1	78.14

From Table 2, it is clear that increasing concentration of the inhibitor resulted in a decrease in corrosion current densities (I_{corr}) and an increase in inhibition efficiency ($E_1\%$), reaching its maximum value, 78.14%, at 2 g/L. This behaviour suggests that the inhibitor adsorption protective film formed on the carbon steel surface tends to be more and more complete and stable. The presence of MR oil caused a slight shift of corrosion potential towards the negative values compared to that in the absence of inhibitor. In literature, it has been also reported that if the displacement in E_{corr} is >85 mV the inhibitor can be seen as a cathodic or anodic type inhibitor and if the displacement of E_{corr} is <85 mV, the inhibitor can be seen as mixed type [27]. In our study, the maximum displacement in E_{corr} value was 15 mV for MR oil which indicates that the inhibitors acts as mixed type inhibitor with predominantly control of cathodic reaction.

EIS measurements

The corrosion of mild steel in 1 M HCl solution in the presence of MR oil was investigated by EIS at room temperature after an exposure period of 30 min. Nyquist plots for mild steel obtained at the interface in the absence and presence of MR oil at different concentrations is given in Fig. 2.

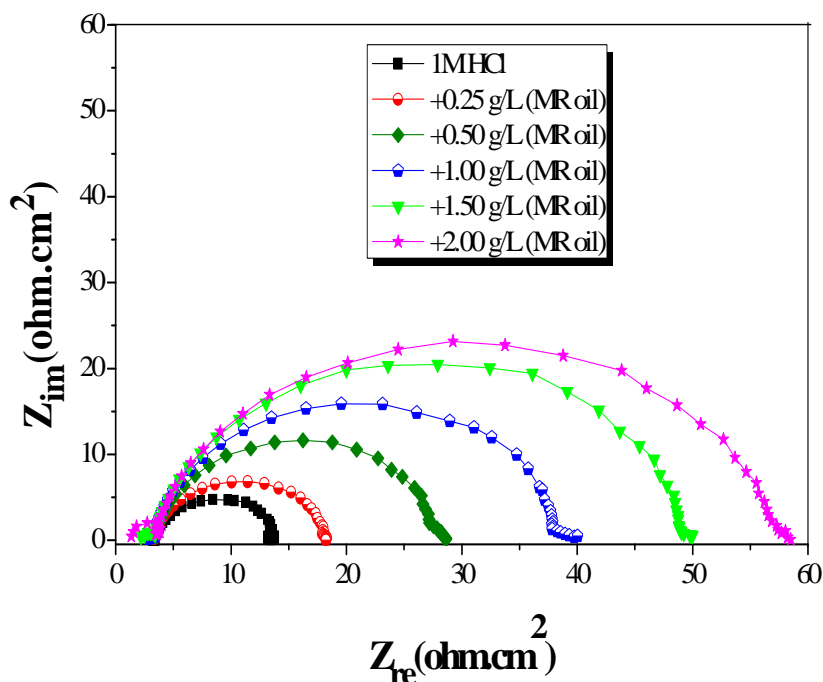


Fig. 2. Nyquist plots for mild steel in 1 M HCl in the presence and absence of different concentrations of *Mentha rotundifolia* essential oil

As shown in Fig. 2, in uninhibited and inhibited 1 M HCl solutions, the impedance spectra exhibit one single capacitive loop, which indicates that the corrosion of steel is mainly controlled by the charge transfer process [28]. It is noted that these capacitive loops in 1 M HCl solutions are not perfect semicircles which can be attributed to the frequency dispersion effect as a result of the roughness and inhomogeneous of electrode surface [29]. Furthermore,

the diameter of the capacitive loop in the presence of inhibitor is larger than that in blank solution, and enlarges with the inhibitor concentration. This indicates that the impedance of inhibited substrate increases with the inhibitor concentration, and leads to good inhibitive performance.

The EIS results of these capacitive loops are simulated by the equivalent circuit shown in Fig. 3 to pure electric models that could verify or rule out mechanistic models and enable the calculation of numerical values corresponding to the physical and/or chemical properties of the electrochemical system under investigation [30]. In the electrical equivalent circuit, R_s is the electrolyte resistance, R_t the charge transfer resistance and C_{dl} is the double layer capacitance.

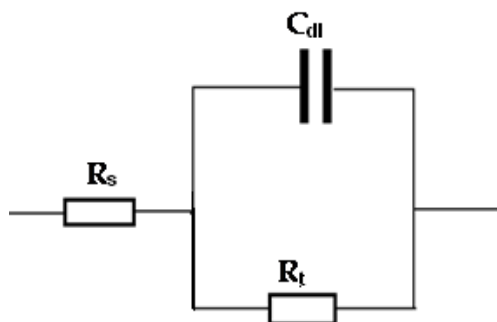


Fig. 3. Equivalent circuit used to fit the EIS data of mild steel in 1 M HCl without and with different concentrations of *Mentha rotundifolia* essential oil

The electrochemical parameters of R_t , C_{dl} and f_{max} derived from Nyquist plots and inhibition efficiency E_{Rt} (%) are calculated and listed in Table 3.

Table 3 Electrochemical parameters for mild steel in 1 M HCl in the presence and absence of different concentrations of *Mentha rotundifolia* essential oil

C (g/L)	E_{corr} (mV/SCE)	R_t ($\Omega \cdot \text{cm}^2$)	f_{max} (Hz)	C_{dl} ($\mu\text{F} \cdot \text{cm}^2$)	E_{Rt} %
0	-512.12	11.35	238.96	58.71	--
0.25	-527.8	17.84	158.71	56.24	36.38
0.50	-528	24.07	132.31	50.00	52.85
1.00	-526.91	37.43	94.75	44.90	69.68
1.50	-527	47.32	76.29	44.11	76.01
2.00	-527.84	54.48	69.51	42.05	79.17

From the impedance data (Table 3), it was clear that:

- (i) R_t values in the presence of the MR oil were always greater than their values in the absence of the inhibitor molecules. This indicates that, this inhibitor was acting as adsorption inhibitor;
- (ii) charge transfer resistance, R_t , values were increased in the presence of the inhibitor and consequently the inhibition efficiency (E_{Rt} %) increases to 79.17% at 2 g/L, which indicates a reduction in the steel corrosion rate;
- (iii) values of double layer capacitance, C_{dl} , are also brought down to the maximum extent in the presence of inhibitor ($42.05 \mu\text{F} \cdot \text{cm}^2$ at 2 g/L) and the decrease in the values of C_{dl} follows the order similar to that obtained for I_{corr} in this study.

Weight loss measurement

The non-electrochemical technique of weight loss was done in order to determine the corrosion rate (W_{corr}) and percentage of inhibition (E_w) at various concentrations of MR oil and at different temperatures (Table 4).

Table 4 Corrosion Parameters for mild Steel in 1 M HCl in absence and presence of different concentrations of *Mentha rotundifolia* essential oil obtained from Weight Loss Measurements at different temperatures

C (g/L)	303 K		313 K		323 K		333 K		343 K	
	W_{corr} (mg/cm ² .h)	E_w (%)								
0	4.178		7.418		11.177		17.369		19.369	
0.25	1.540	63.14	2.925	60.57	4.695	58	7.795	55.12	9.845	49.17
0.5	1.357	67.52	2.536	65.82	4.328	61.28	7.224	58.41	8.487	56.18
1.00	1.088	73.96	2.058	72.26	3.371	69.84	5.645	67.5	7.023	63.74
1.50	1.032	75.31	1.901	74.38	3.114	72.14	5.192	70.11	6.754	65.13
2.00	0.882	78.88	1.629	78.04	2.691	75.93	4.799	72.37	5.787	70.12

Effect of MR oil on corrosion rate (W_{corr})

The corrosion rate (W_{corr}) obtained of mild steel in the absence and in the presence of various concentrations of MR oil at different temperatures in 1 M HCl solutions after 6 h of immersion are shown in Fig. 4.

304
305
306

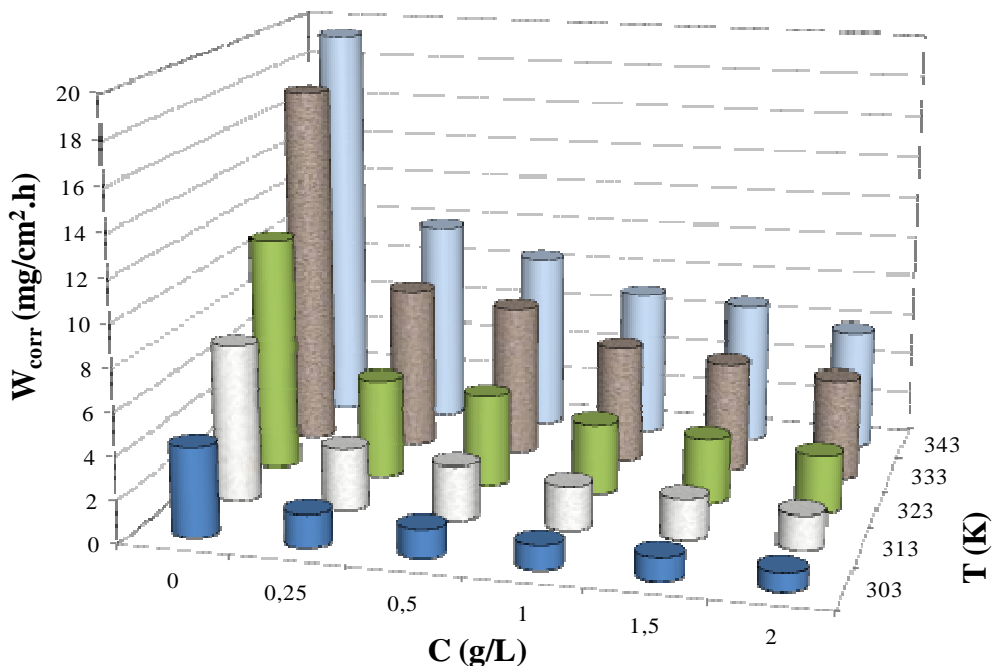


Fig. 4. Variation of W_{corr} as a function of temperature and concentration of *Mentha rotundifolia* essential oil

The results indicated that the corrosion rate (W_{corr}) of mild steel decreased continuously with increasing the inhibitor concentration, ie, the corrosion of steel is retarded by MR oil, or the inhibition enhances with the inhibitor concentration. This behaviour is due to the fact that the adsorption coverage of inhibitor on steel surface increases with the inhibitor concentration. Also, the corrosion rate (W_{corr}) increases with temperature both in uninhibited and inhibited solutions, especially goes up more rapidly in the absence of inhibitor. These results confirm that MR oil acts as an effective inhibitor in the range of temperature studied.

307
308
309
310
311
312
313
314
315
316
317
318
319

Effect of MR oil on inhibition efficiency (E_w)

The values of E_w for different MR oil concentrations at 303-343 K in 1 M HCl solution are presented in Fig. 5.

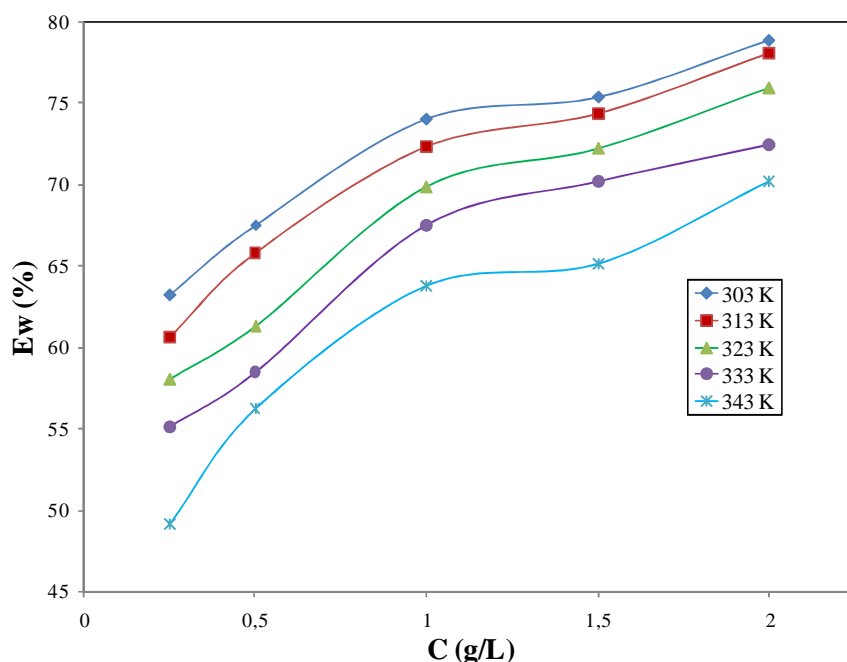


Fig. 5. Relationship between inhibition efficiency (E_w) and temperature and concentration of *Mentha rotundifolia* essential oil in 1 M HCl

320
321

The results reveal that inhibition efficiency E_w increases sharply with increase in concentration of inhibitor, indicating that the extent of inhibition is dependent on the amount of MR oil (concentration-dependent). Also, we note that the efficiency (E_w) depends on the temperature and decreases with the rise of temperature from 303 to 343 K, and when the concentration reached to 2 g/L, E_w of MR oil reached a high values of 78.88% in 1 M HCl solution at 303 K, which represents excellent inhibitive ability of MR oil. The decrease in inhibition efficiency with increase in temperature may be attributed to the increased desorption of inhibitor molecules from metal surface and the increase in the solubility of the protective film or the reaction products precipitated on the surface of the metal that might otherwise inhibit the reaction. This is in accordance with our previous results [7-9].

The variation of inhibition efficiency (E %), determined by the three methods (weight loss, polarization curves and EIS methods), as a function of concentration of MR oil in 1 M HCl show a good agreement with the three methods used in this investigation, significantly in high concentrations.

Kinetic/Activation parameters

In order to calculate activation parameters of the corrosion reaction such as activation energy $E^{\circ a}$, activated entropy $\Delta S^{\circ a}$ and activation enthalpy $\Delta H^{\circ a}$ for the corrosion of mild steel in acid solution in absence and presence of different concentrations of MR oil, the Arrhenius equation (7) and its alternative formulation called transition state equation (8) were employed [31].

$$W = A \exp\left(-\frac{E_a^{\circ}}{RT}\right) \quad (7)$$

$$W = \frac{RT}{Nh} \exp\left(\frac{\Delta S_a^{\circ}}{R}\right) \exp\left(-\frac{\Delta H_a^{\circ}}{RT}\right) \quad (8)$$

where $E^{\circ a}$ is the apparent activation corrosion energy, T is the absolute temperature, R is the universal gas constant, A is the Arrhenius pre-exponential factor, h is he Plank's constant, N is the Avogrado's number, $\Delta S^{\circ a}$ is the entropy of activation and $\Delta H^{\circ a}$ is the enthalpy of activation.

Plotting the logarithm of the corrosion rate (W_{corr}) versus reciprocal of absolute temperature, the activation energy can be calculated from the slope ($-E^{\circ a}/R$). Fig. 6 shows the variations of $\ln(W_{\text{corr}})$ with the presence and absence of inhibitor with the (1/T).

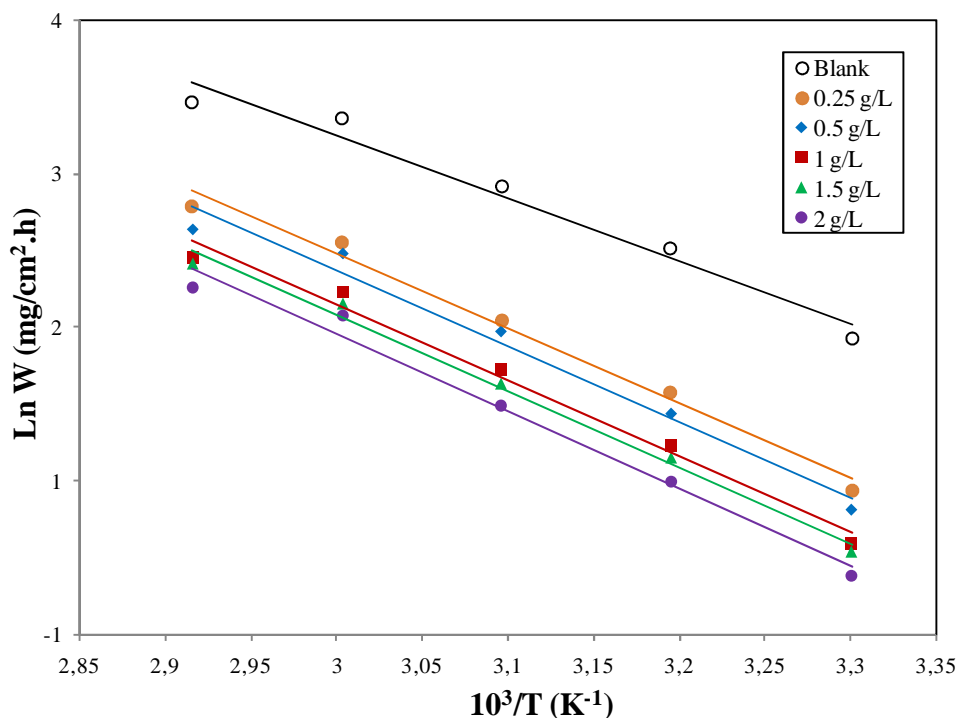


Fig. 6. Arrhenius plots for mild steel corrosion rates (W_{corr}) in 1 M HCl in the absence and presence of different concentrations of *Mentha rotundifolia* essential oil

The logarithm of the corrosion rate of steel $\ln(W_{\text{corr}})$ can be represented as straight-lines function of $(10^3/T)$ with the linear regression coefficient (R^2) was close to 1, indicating that the corrosion of steel in hydrochloric acid without and with inhibitor follows the Arrhenius equation. The activation energy (E°_a) values were calculated from the Arrhenius plots (Fig. 6) and the results are shown in Table 5.

Further, using Eq. (8), plots of $\ln(W_{\text{corr}}/T)$ versus $10^3/T$ gave straight lines (Fig. 7) with a slope of $(-\Delta H^{\circ}_a/R)$ and an intercept of $(\ln(R/Nh) + (\Delta S^{\circ}_a/R))$ from which the values of ΔH°_a and ΔS°_a were calculated and are listed in Table 5.

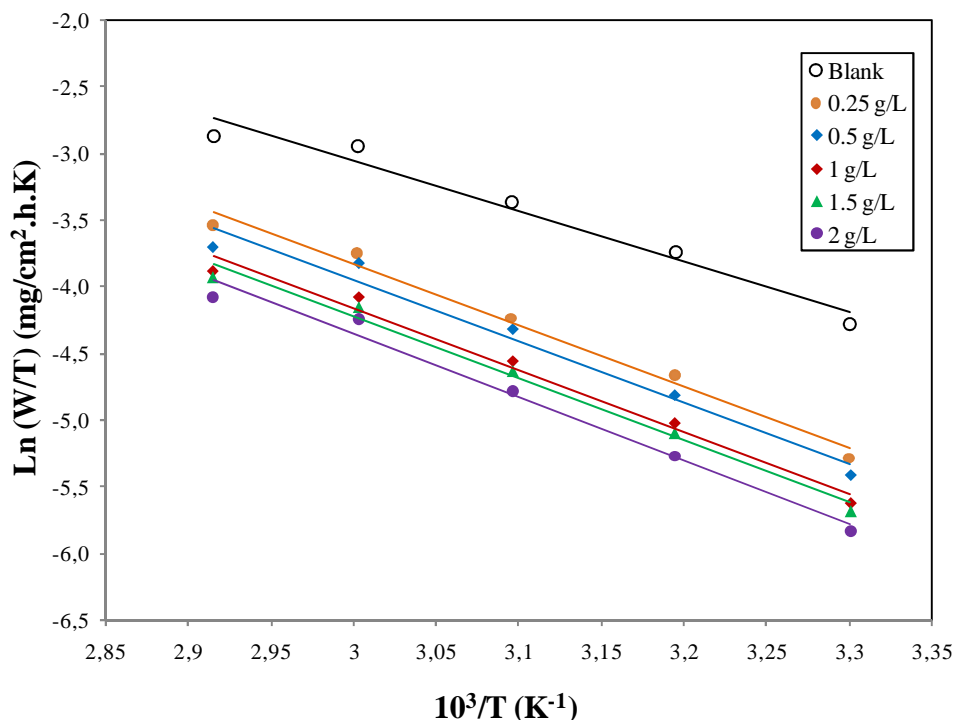


Fig. 7. Transition-state plot for mild steel corrosion rates (W_{corr}) in 1 M HCl in absence and presence of different concentrations of *Mentha rotundifolia* essential oil

The activation energies in the presence of MR oil were observed higher than those in uninhibited acid solution (Table 5). This explains that the energy barrier of corrosion reaction increases with the concentration of MR oil. It is clear from equation (7) that corrosion rate is influenced by E°_a . Generally, higher E°_a value leads to the lower corrosion rate. In addition, the value of activation energy that is around 40–80 KJ.mol^{-1} can be suggested to obey the physical adsorption (physisorption) mechanism [32]. Physisorption is often related with this phenomenon, where an adsorptive film of electrostatic character is formed on the mild steel surface.

Table 5 Activation parameters E°_a , ΔS°_a , ΔH°_a of the dissolution of mild steel in 1 M HCl in the absence and presence of different concentrations of *Mentha rotundifolia* essential oil

C (g/L)	E°_a (KJ.mol^{-1})	ΔH°_a (KJ.mol^{-1})	$E^{\circ}_a - \Delta H^{\circ}_a$ (KJ.mol^{-1})	ΔS°_a ($\text{J.mol}^{-1}.\text{K}^{-1}$)
0	34.09	31.41	2.68	-128.88
0.25	40.73	38.06	2.67	-115.40
0.50	40.98	38.30	2.68	-115.60
1.00	41.15	38.48	2.67	-116.89
1.50	41.33	38.65	2.68	-116.92
2.00	42.04	39.36	2.68	-115.87

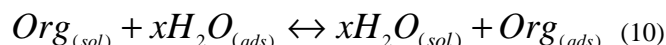
The positive value of enthalpy of activation (ΔH°_a) in the absence and presence of various concentration of inhibitor reflects the endothermic nature of mild steel dissolution process meaning that dissolution of steel is difficult [33]. It is evident from the table that the value of ΔH°_a increased in the presence of the inhibitor than the uninhibited solution indicating higher protection efficiency. This may be attributed to the presence of energy barrier for the reaction; hence the process of adsorption of inhibitor leads to rise in enthalpy of the corrosion process. The negative values of entropies of activation (ΔS°_a) imply that the activated complex in the rate determining step represents an association rather than a dissociation step, meaning that a decrease in disordering takes place on going from reactants to the activated complex [34].

On the other hand, the average difference value of the $E^{\circ}a - \Delta H^{\circ}a$ is 2.68 KJ.mol^{-1} , which is approximately equal to the average value of RT (2.69 KJ.mol^{-1}) at the average temperature (323 K) of the domain studied. This result agrees that the corrosion process is a unimolecular reaction as described by the known Eq. (9) of perfect gas:

$$E^{\circ}a - \Delta H^{\circ}a = RT \quad (9)$$

Adsorption isotherm and Thermodynamic parameters

It is known that the adsorption process of inhibitor depends on its electronic characteristics, the nature of metal surface, temperature, steric effects and the varying degrees of surface-site activity. In fact, the solvent H_2O molecules could also be adsorbed at the metal/solution interface. In the aqueous solution, the adsorption of inhibitor molecules can be considered as a quasi-substitution process between the inhibitor in the aqueous phase $\text{Inh}_{(\text{sol})}$ and water molecules at the electrode surface $\text{H}_2\text{O}_{(\text{ads})}$ [35]:



where x is the size ratio, that is, the number of water molecules re-placed by one organic inhibitor.

This equation showed that the interaction force between metal and inhibitor must be greater than the interaction force of metal and water molecule. The corrosion adsorption processes can be understood using adsorption isotherm. Langmuir adsorption isotherm is attributing to physisorption or chemisorption phenomenon while Temkin adsorption isotherm gives an explanation about the heterogeneity formed on the metal surface. Chemisorption is attributed to Temkin isotherm [36]. Here, Langmuir, Frumkin and Temkin adsorption isotherms were applied in order to explain the adsorption process of MR oil on the mild steel surface:

$$\text{Langmuir} : \frac{C_{\text{inh}}}{\theta} = \frac{1}{K} + C_{\text{inh}} \quad (11)$$

$$\text{Temkin} : \text{Ln} \left(\frac{C_{\text{inh}}}{\theta} \right) = \text{Ln}K - g\theta \quad (12)$$

$$\text{Frumkin} : \text{Ln} \left(C_{\text{inh}} * \left(\frac{\theta}{1-\theta} \right) \right) = \text{Ln}K + g\theta \quad (13)$$

where θ is the surface coverage, K is the adsorption-desorption equilibrium constant, C_{inh} is the concentration of inhibitor and g is the adsorbate parameter.

The dependence of the fraction of the surface covered θ obtained by the ratio $E_w/100$ as function of the MR oil concentration (C_{inh}) was graphically fitted for these various adsorption isotherms.

The linear regression parameters between C/θ and C are listed in Table 6, and the straight lines of C/θ versus C in 1 M HCl at different temperatures are shown in Fig. 8. It is evident that all linear correlation coefficients (R^2) are almost equal to 1, and the slope values are also close to 1, which indicates that the adsorption of MR oil on steel surface obeys Langmuir adsorption isotherm. This result showed that the adsorbed molecules occupy only one site and there are no interactions with other adsorbed species [37].

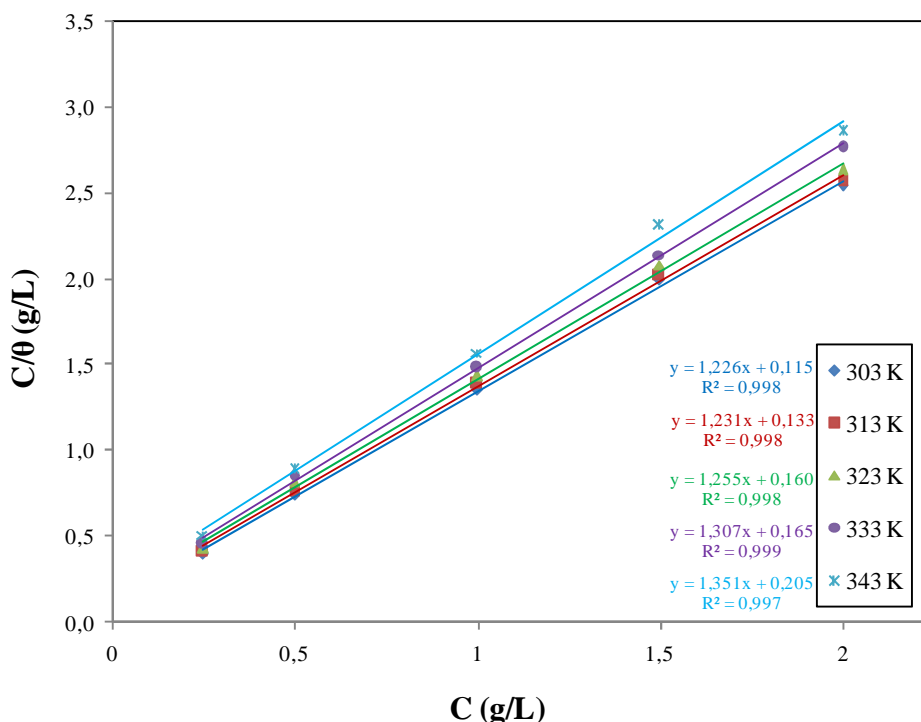


Fig. 8. Langmuir adsorption isotherm of *Mentha rotundifolia* essential oil on the mild steel surface in 1 M HCl at different temperatures

As shown in Table 6, the adsorptive equilibrium constant (K) decreases with the temperature in 1 M HCl solution, which could be ascribed to that it is easy for inhibitor to adsorb on the steel surface at relatively lower temperature. But when the temperature is gone up, the adsorbed inhibitor tends to desorb from the steel surface. Generally, large value of K is bound up with better inhibition efficiency of a given inhibitor. This is in good agreement with the values of E_w obtained from Fig. 5.

Thermodynamic parameters are important to further understand the adsorption process of inhibitor on steel/solution interface. The equilibrium adsorption constant, K is related to the standard Gibbs free energy of adsorption (ΔG_{ads}°) with the following equation:

$$K = \frac{1}{55.5} \cdot \exp\left(-\frac{\Delta G_{ads}^\circ}{RT}\right) \quad (14)$$

The standard adsorption enthalpy (ΔH_{ads}°) could be calculated on the basis of Van't Hoff equation [38]:

$$\ln K = -\frac{\Delta H_{ads}^\circ}{RT} + D \quad (15)$$

where R is the universal gas constant, T is the thermodynamic temperature, D is integration constant, and the value of 55.5 is the concentration of water in the solution in mol/L (10^3 g/L).

The standard adsorption enthalpy (ΔH_{ads}°) can also be calculated from the Gibbs-Helmholtz equation:

$$\frac{\Delta G_{ads}^\circ}{T} = \frac{\Delta H_{ads}^\circ}{T} + k \quad (16)$$

To calculate the enthalpy of adsorption (ΔH_{ads}°), $\ln K$ was plotted against $1/T$ (Fig. 9) and straight line was obtained with slope equal to $(-\Delta H_{ads}^\circ/T)$. The variation of $\Delta G_{ads}^\circ/T$ vs $1/T$ gives straight line with slope equal to ΔH_{ads}° (Fig. 10).

429

430

431

432

433

434

435

436

437

438

439

440

441

442

443

444

445

446

447

448

449

450

451

452

453

454

455

456

457

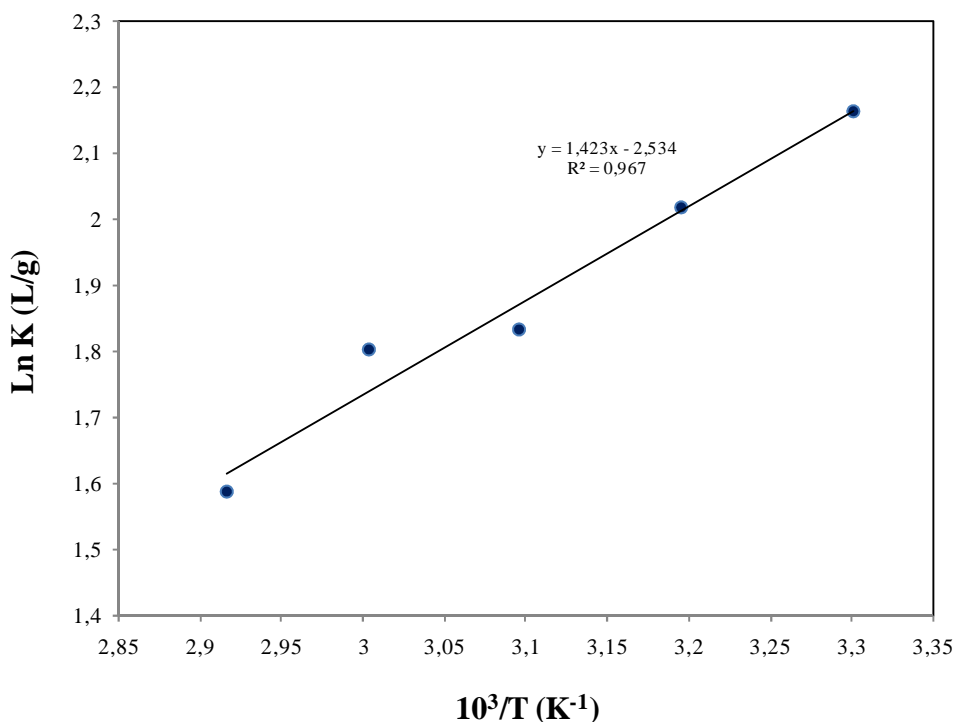


Fig. 9. Van't Hoff's plot of Ln K against 1/T for the adsorption of *Mentha rotundifolia* essential oil onto mild steel

458
459
460

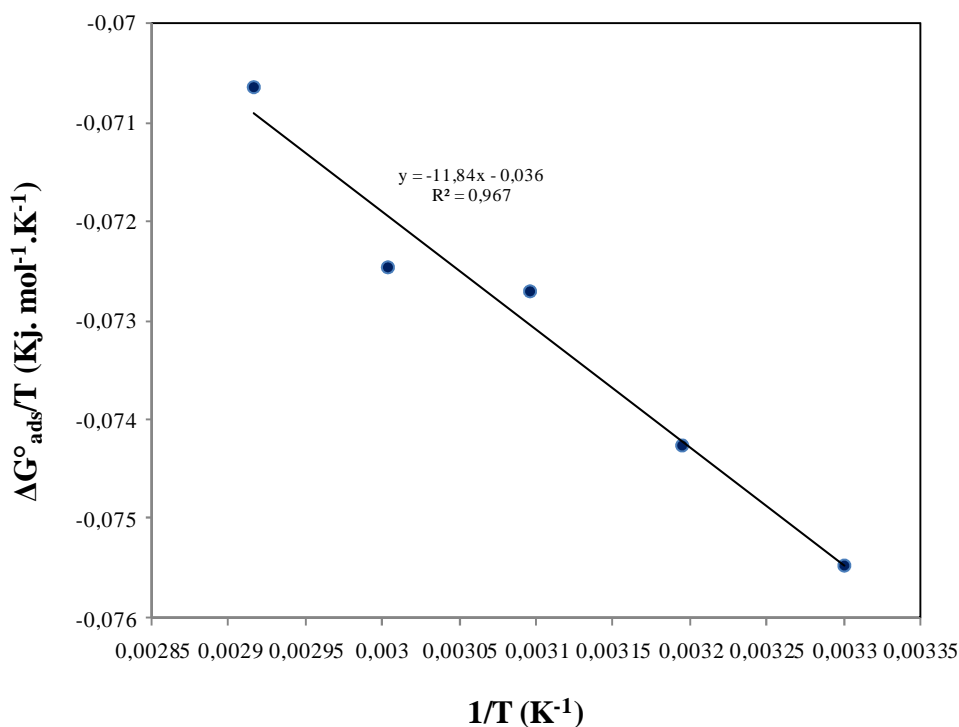


Fig. 10. The relationship between (ΔG°_ads/T) and 1/T

461
462
463
464
465
466

With the obtained both parameters of ΔG°_ads and ΔH°_ads, the standard adsorption entropy (ΔS°_ads) can be calculated using the following thermodynamic basic Equ. (17). All the standard thermodynamic parameters are listed in Table 6.

$$\Delta S^{\circ}_{ads} = \frac{\Delta H^{\circ}_{ads} - \Delta G^{\circ}_{ads}}{T} \quad (17)$$

467
468
469
470
471

Table 6 Thermodynamic parameters for adsorption of *Mentha rotundifolia* essential oil on mild steel in 1 M HCl solution at different temperatures from Langmuir adsorption isotherm

Temperature (K)	R ²	K (L/g)	$\Delta G^{\circ}_{\text{ads}}$ (KJ.mol ⁻¹)	$\Delta H^{\circ}_{\text{ads}}$ (KJ. mol ⁻¹)	$\Delta S^{\circ}_{\text{ads}}$ (J.mol ⁻¹ .K ⁻¹)
303	0.998	8.69	-22.86	-11.84	36,39
313	0.998	7.52	-23.24		36,43
323	0.998	6.25	-23.49		36,06
333	0.999	6.06	-24.13		36,91
343	0.997	4.88	-24.24		36,14

The negative values of $\Delta G^{\circ}_{\text{ads}}$ suggest (Table 6) that the adsorption of inhibitor molecules onto steel surface is a spontaneous phenomenon. It is well known that values of $\Delta G^{\circ}_{\text{ads}}$ around -20 KJ.mol^{-1} or lower are associated with the physisorption phenomenon where the electrostatic interaction assemble between the charged molecule and the charged metal, while those around -40 KJ.mol^{-1} or higher are associated with the chemisorption phenomenon where the sharing or transfer of organic molecules charge with the metal surface occurs [39]. In the present study, the value of $\Delta G^{\circ}_{\text{ads}}$ computed and shown in Table 5 supports the physisorption of MR oil on mild steel.

Also, the negative values of $\Delta H^{\circ}_{\text{ads}}$ mean that the dissolution process is an exothermic phenomenon. The exothermic process is attributed to either physical or chemical adsorption or mixture of both whereas endothermic process corresponds to chemisorptions [40,41]. In an exothermic process, physisorption is distinguished from chemisorption by considering the absolute value of $\Delta H^{\circ}_{\text{ads}}$. For physisorption process, the value of $\Delta H^{\circ}_{\text{ads}}$ is lower than 40 KJ.mol^{-1} while the heat of adsorption for chemisorption process is approaches to 100 KJ.mol^{-1} [40]. In our study, the heat of adsorption is $-11.84 \text{ KJ.mol}^{-1}$ postulates that a physisorption is more favoured. The value of the enthalpy of adsorption found by the two methods such as Van't Hoff and Gibbs–Helmholtz relations are in good agreement.

Moreover, the positive value of $\Delta S^{\circ}_{\text{ads}}$ (around $36 \text{ J.mol}^{-1}.\text{K}^{-1}$) in the presence of inhibitor is an indication of increase in solvent entropy. It also interpreted with increase of disorders due to more water molecules which can be desorbed from the metal surface by one inhibitor molecule. Therefore, it is revealed that decrease in the enthalpy is the driving force for the adsorption of the inhibitor on the surface of the metal [42].

Explanation for inhibition

The MR essential oil was dominated by pulegone (69.1%) and menthone (18.5%). These compounds represent 87.6% of the total oil and contain oxygen atoms in functional groups (C=O) and π -electrons of the double bonds (C=C), which meets the general characteristics of typical corrosion inhibitors. Accordingly, the inhibitive action of MR oil could be attributed to the adsorption of these oxygenated compounds on the mild steel surface [43]. However, it is also possible that the minor components might be involved in some type of synergism effect with these two compounds.

Generally, in aqueous acidic solution, the organic molecules of MR essential oil exist either as neutral molecules or in the form of protonated organic molecules (cations). Therefore, two modes of adsorption are considered on the metal surface in acid media. In the first mode, the neutral molecules may be adsorbed on the surface of mild steel through the chemisorption mechanism, involving the displacement of water molecules from the mild steel surface and the sharing electrons between the oxygen atoms and iron. The inhibitor molecules can also adsorb on the mild steel surface on the basis of donor–acceptor interactions between their π -electrons and vacant d-orbitals of surface iron. In second mode, since it is well known that it is difficult for the protonated molecules to approach the positively charged mild steel surface (H_3O^+ /metal interface) due to the electrostatic repulsion. Since Cl^- have a smaller degree of hydration, they could bring excess negative charges in the vicinity of the interface and favour more adsorption of the positively charged inhibitor molecules, the protonated inhibitors adsorb through electrostatic interactions between the positively charged molecules and the negatively charged metal surface. Thus, there is a synergism between adsorbed Cl^- ions and protonated inhibitors [44,45].

CONCLUSION

Mentha rotundifolia essential oil acts as good inhibitor for the corrosion of mild steel in 1M HCl solution. The inhibition action of this essential oil can be attributed to the adsorption of major oxygenated monoterpenic compounds as pulegone and menthone. The results of potentiodynamic measurements revealed clearly that MR oil is a good cathodic inhibitor for mild steel corrosion in acidic solution. The results of EIS measurements indicated that the corrosion of steel is mainly controlled by the charge transfer process. From loss measurements, is clear that inhibition efficiency values increased with increase in inhibitor concentration but decreased with increase in temperature. The value of apparent activation energy increased with the increase in the inhibitor concentration. Enthalpy of activation reflects the endothermic nature of the mild steel dissolution process. Entropy of activation

increased with increasing inhibitor concentration; hence increase in the disorderliness of the system. The adsorption behavior can be described by the Langmuir adsorption isotherm. Gibbs free energy of adsorption, enthalpy of adsorption and entropy of adsorption indicated that the adsorption process is spontaneous and exothermic and the molecules adsorbed on the metal surface by the process of physical adsorption.

REFERENCES

- [1] B.A. Shaw, R.G. Kelly, *Electroch. Soc. Interf.* **2006**, 15, 24.
- [2] M.A. Quraishi, S. Khan. *J Appl. Electrochem.* **2006**, 5, 539.
- [3] I.B. Obot, N.O. Obi-Egbedi. *J. Appl. Electrochem.* **2010**, 11, 1977.
- [4] A. Bouyanzer, B. Hammouti, L. Majidi, *Mater. Letters* **2006**, 60, 2840.
- [5] A. Bouyanzer, L. Majidi, B. Hammouti, *Bull. Elect.* **2006**, 22, 321.
- [6] O. Ouachikh, A. Bouyanzer, M. Bouklah, J-M. Desjobert, J. Costa, B. Hammouti, L. Majidi *Surf. Rev. Lett.* **2009**, 16, 49.
- [7] G. Cristofari, M. Znini, L. Majidi, A. Bouyanzer, S. Al-Deyab, J. Paolini, B. Hammouti, J. Costa, *Int J. Electrochem. Sci.* **2011**, 6, 6699.
- [8] M. Manssouri, M. Znini, A. Ansari, A. Bouyanzer, Z. Faska, L. Majidi *Der Pharma Chemica* **2014**, 6, 331.
- [9] Y. El Ouadi, A. Bouyanzer, L. Majidi, J. Paolini, J. M. Desjobert, J. Costa, A. Chetouani and B. Hammouti, *J. Chem. Pharmac. Res.* **2014**, 6, 1401.
- [10] M. Znini, L. Majidi, A. Bouyanzer, J. Paolini, J.M. Desjobert, J. Costa, B. Hammouti, *Arab J. Chem.* **2012**, 5, 467.
- [11] M. Manssouri, Y. El Ouadi, M. Znini, J. Costa, A. Bouyanzer, J.M. Desjobert, L. Majidi *J. Mater. Environ. Sci.* **2015**, 6, 631.
- [12] A.O. Tucker, R.F.C. Naczi, *Mentha: an overview of its classification and relationships.* (In: Lawrence BM (ed) *Mint: the genus Mentha*, CRC Press, **2007**) 3.
- [13] D. Lorenzo, D. Paz, E. Dellacassa, P. Davies, R. Vila, S. Canigueral, *Arch. Biol. Tech.* **2002**, 45, 125.
- [14] A. Idrissi, J. Bellakhdar, *Al Biruniya.* **1989**, 5, 79.
- [15] E. Derwich, Z. Benziane, A. Boukir, *EJEAFCh.* **2010**, 9, 19.
- [16] European Pharmacopoeia, Council of Europe, 3rd edn. (Strasbourg, 1997), pp. 121-122
- [17] H. Dool, P. Kratz, *J. Chromat.* **1963**, 11, 463.
- [18] D. Joulain, W. König, *The atlas of spectral data of sesquiterpene hydrocarbons.* EbVerlag, Hamburg, **1989**.
- [19] D. Hochmuth, D. Joulain, W. König. *Terpenoids and related constituents of essential oils.* Library of Massfinder, Hamburg, **2001**.
- [20] R.P. Adams, *Identification of essential oil components by Gas chromatography/quadrupole mass spectroscopy.* Allured Publishing, Carol Stream, **2001**.
- [21] T. Tsuru, S. Haruyama, B. Gijutsu. *Jpn Soc Corros Eng.* **1978**, 27, 573.
- [22] A. Nagell, F. Hefendehl, *Planta Med.* **1974**, 26, 1.
- [23] M. Brada, M. Bezzina, M. Marlier, A. Carlier, G. Lognay, *Biotechnol Agron Soc Environ.* **2007** 11, 3.
- [24] S. Kokkini, V.P. Papageorgiou, *Planta Med.* **1988**, 38, 166.
- [25] M.D. Pérez Raya, M.P. Utrilla, M.C. Navarro, J. Jimén. *Phytoh. Res.* **1990** 4, 232.
- [26] R. Croteau, J. Gershenzon, B.E. Ellis, G.W. Kuroki, H.A. Stafford, (New York, **1994**), p. 183
- [27] A.K. Satapathy, G. Gunasekaran, S.K. Sahoo, K. Amit, P.V. Rodrigues, *Corros. Sci.* **2009**, 51, 2848.
- [28] A.R. Sathiyapriya, V.S. Muralidharan, Subramanian. *Corrosion.* **2008**, 64, 541.
- [29] F. Mansfel, M.W. Kendig, S. Tsai, *Corrosion.* **1982**, 38, 570.
- [30] M. Benabdellah, A. Aouniti, A. Dafali, B. Hammouti, M. Benkaddour, A. Yahyi, A. Ettouhami, *Appl. Surf Sci.* **2006**, 252, 8341.
- [31] F. Bentiss, M. Traisnel, M. Lagrenée, *Corros. Sci.* **2000**, 42, 127.
- [32] K.O. Orubite, N.C. Oforka, *Mater. Lett.* **2004**, 58, 1768.
- [33] N.M. Guan, L. Xueming, L. Fei, *Chem. Phys.* **2004**, 86, 59.
- [34] S. Samkarapapaavinasam, M.F. Ahmed, *J. Appl. Electrochem.* **1992**, 22, 390.
- [35] I. El Ouali, B. Hammouti, A. Aouniti, Y. Ramli, M. Azougagh, E.M. Essassi, M. Bouachrine, *J. Mater. Environ. Sci.* **2010**, 1, 1.
- [36] D. Wahyuningrum, S. Achmad, Y. Syah, B. M Buchari, B. Bundjali, B. Ariwahjoedi, *In J. Electrochem. Sci.* **2008**, 3, 154
- [37] S. Cheng, S. Chen, T. Liu, X. Chang, Y. Yin, *Mater Lett.* **2007**, 61, 3276
- [38] T. Libin, M. Guannan, L. Guangheng, *Corros. Sci.* **2003**, 45, 2251.
- [39] E. Khamis, F. Bellucci, R. Latanision, E.S. El-Ashry, *Corrosion.* **1991**, 47, 677.
- [40] F. Bentiss, M. Lebrini, M. Lagrenée, *Corros. Sci.* **2005**, 47, 2915.
- [41] S.F. Mertens, C. Xhoffer, B.C. Decooman, Temmerman, *Corrosion.* **1997**, 53, 381.
- [42] A. Gulsen, *Coll Surf.* **2008**, 317, 730.

-
- [43] Z. Faska, A. Bellioua, M. Bouklah, L. Majidi, R. Fih, A. Bouyanzer, B. Hammouti, *Monatsh. Chem.* 2008, 139, 1417. 587
- [44] G.N. Mu, T.P. Zhao, M. Liu, T. Gu, *Corrosion.* **1996**, 52, 853. 588
- [45] I. Ahamad, S. Khan, K.R. Ansari, Quraishi. *J. Chem. Pharm. Res.* **2011**, 3, 703. 589
- [46] Knowledge: This work was done within the framework of the FP7 IRSES project Oil & Sugar project (contract No. 295202) which supported mobility of young researchers between the partners participating to it. 590
- 591
- 592